from regular Gaussian rings.[8-11] After multiplying of all three components, one obtains

$$w_3(R_{kl}) \sim \exp\left\{-\frac{3}{2b^2\mu'}\left[\frac{\mu' L^2}{2N} + \frac{2N\mu'}{2\mu' N - (l+k-2N)^2}\left(\frac{L^2 n^2}{4N^2} - \frac{n}{N} L R_{kl} \cos\vartheta + R_{kl}^2\right)\right]\right\} \quad \text{(A11)}$$

Averaging over all $\sin\vartheta\, d\vartheta$ and using ν from eq 11 leads to

$$W_3(R_{kl}) \sim \exp\left\{-\frac{3}{2b^2\mu'}\left[\frac{\mu' L^2}{2N} + \frac{\nu n^2 L^2}{4N^2} + \nu R_{kl}^2\right]\right\} \times 2\frac{\sinh\{3\nu n L R_{kl}/2N\mu' b^2\}}{3\nu n L R_{kl}/2N\mu' b^2} \quad \text{(A12)}$$

Normalization of eq A12 over $d\varphi R_{kl}^2\, dR_{kl}$ finally results in

$$W_3(R_{kl}) = 2\left(\frac{3\nu}{2b^2\pi\mu'}\right)^{3/2} \exp\left\{-\frac{3L^2\nu n^2}{8b^2N^2\mu'}\right\} \exp\left\{-\frac{3\nu R_{kl}^2}{2b^2\mu'}\right\} \times \frac{\sinh\{3L\nu n R_{kl}/2b^2 N\mu'\}}{(3L\nu n R_{kl}/2b^2 N\mu')} \quad \text{(A13)}$$

References and Notes

(1) Lord Rayleigh *Philos. Mag.* **1919**, *37*, 321.
(2) Kratky, O.; Porod, G. *Recl. Trav. Chim. Pays-Bas* **1949**, *68*, 1106.
(3) Doolittle, R. F. *Annu. Rev. Biochem.* **1984**, *53*, 195, references therein.
(4) Muroga, Y. *Macromolecules* **1988**, *21*, 2751.
(5) Wenzel, M.; Ballauff, M.; Wegner, G. *Makromol. Chem.* **1987**, *188*, 2865.
(6) Gradshteyn, I. S.; Ryzhik, I. M. *Table of Integrals, Series, and Products*; Academic Press: New York, San Francisco, London, 1965.
(7) Chandrasekhar, S. *Rev. Mod. Phys.* **1943**, *15*, 1.
(8) Zimm, B.; Stockmayer, W. H. *J. Chem. Phys.* **1949**, *17*, 1301.
(9) Casassa, E. F. *J. Polym. Sci., Part A* **1965**, *3*, 605.
(10) Yamakawa, H. *Modern Theory of Polymer Solutions*; Harper & Row: New York, Evanston, San Francisco, London, 1971; Sec. 9b.
(11) Burchard, W. In *Cyclic Polymers*, Semlyen, J. A. Ed.; Elsevier: London, 1986; Chapter 2.
(12) Fukatsu, M.; Kurata, M. *J. Chem. Phys.* **1966**, *44*, 4539.
(13) Debye, P. In *Light Scattering from Dilute Polymer Solutions*; McIntyre, D., Eds.; Gormick, F., Eds.; Gordon and Breach: New York, London, 1964; p 139.
(14) Kirkwood, J. G.; Riseman, J. *J. Chem. Phys.* **1948**, *16*, 565.
(15) Abramowitz, M.; Stegun, I. A. *Handbook of Mathematical Functions*; Dover: New York, p 295.
(16) Numerical calculations were performed with subprograms of the *IMSL LIBRARY* and *IMSL SFUN/LIBRARY*, IMSL, Inc., Houston, TX, 1985.
(17) Hadziioannou, G.; Cotts, P. M.; ten Brinke, G.; Han, C. C.; Lutz, P.; Strazielle, P.; Rempp, P.; Kovacs, A. J. *Macromolecules* **1987**, *20*, 493.
(18) Schmidt, M.; Paradossi, G.; Burchard, W. *Macromol. Chem. Rapid Commun.* **1985**, *6*, 767.
(19) Riseman, J.; Kirkwood, J. G. *J. Chem. Phys.* **1950**, *18*, 512.
(20) Bloomfield, V. A.; Zimm, B. *J. Chem. Phys.* **1966**, *44*, 315.
(21) Neugebauer, T. *Ann. Phys.* **1943**, *42*, 509.

Quasi-Elastic and Electrophoretic Light Scattering Studies of the Reorganization of Dioleoylphosphatidylcholine Vesicle Membranes by Poly(2-ethylacrylic acid)

Ki Min Eum,[†] Kenneth H. Langley,*[,†] and David A. Tirrell[‡]

Departments of Physics and Astronomy and Polymer Science and Engineering, University of Massachusetts, Amherst, Massachusetts 01003.

Received May 2, 1988; Revised Manuscript Received December 16, 1988

ABSTRACT: Quasi-elastic light scattering (QELS) and electrophoretic light scattering (ELS) measurements have been used to investigate the pH-dependent structural reorganization of phospholipid vesicles suspended in aqueous solutions of poly(2-ethylacrylic acid) (PEAA). The average radius of dioleoylphosphatidylcholine (DOPC) vesicles suspended in aqueous PEAA was reduced within 1 h from approximately 600 to 60 nm upon acidification. Size distribution analysis revealed narrow single peaks far from the pH at which the reorganization occurs but bimodal distributions in the transition region. The transition pH was shifted from 7.0 to 6.5 as the ionic strength of the sample solutions was increased from 50 to 500 mM. The conformational transition of PEAA from an expanded form at high pH to a relatively compact coil in acidic solutions was also observed by QELS. ELS measurements showed that, as the pH is lowered from 8.0 to 5.5 in the presence of PEAA, the electrophoretic mobility of DOPC vesicles passes through a minimum at the transition pH. At pH lower than that of the transition, vesicle mobility is greater in PEAA solutions than in simple buffers. We believe the increase in mobility is due to adsorption of PEAA on the vesicle surface. We infer that as the pH is lowered, the collapsed PEAA chain provides a hydrophobic site for solubilization of the phospholipid hydrocarbon tails and in so doing disrupts the structural organization characteristic of the pure phospholipid.

Introduction

Surfactant bilayers have been a subject of intense scientific interest for the last 2 decades, since Bangham's[1] illustration of the analogy between such "liposomal" structures and the complex plasma membranes of cells. An essential and intriguing characteristic of the natural membranes is their capacity to respond to signals of various kinds; membrane signaling plays a critical role in intercellular communication, in the binding and processing of ligands and receptors, in energy transduction, and in many other vital cellular processes.

We have explored over the last several years a simple approach to the construction of synthetic bilayer membranes that share this essential capacity to respond to

[†] Department of Physics and Astronomy.
[‡] Department of Polymer Science and Engineering.

0024-9297/89/2222-2755$01.50/0

signals. The approach has used synthetic polyelectrolytes to modify the self-assembly of membrane-forming surfactants and exploited changes in polyelectrolyte hydration and conformation to achieve controlled membrane reorganization.[2-6]

Poly(2-ethylacrylic acid) (PEAA, 1) has proven particularly useful in this regard. Acidification of aqueous

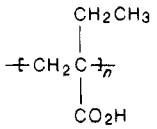

1

solutions of PEAA is accompanied by dehydration of the chain and by a conformational transition from an extended, hydrophilic form to a compact hydrophobic coil.[7-9] In suspensions of natural or synthetic phosphatidylcholines (2), the pH-dependent adsorption of PEAA drives rapid

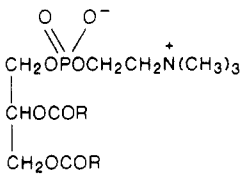

2a, R = $C_{15}H_{31}$
b, R = $C_{17}H_{33}$

membrane reorganization and release of vesicle contents.[3] In the case of dipalmitoylphosphatidylcholine (DPPC, **2a**), the reorganization consists of a transition from a vesicular lipid aggregate at high pH to a mixed polymer–lipid micelle in acidic polymer solutions.[10] Quasi-elastic light scattering reveals a decrease in the average hydrodynamic radius of the lipid aggregates from 90 to 5.5 nm upon acidification, and negative-stain electron microscopy shows only disklike micelles at low pH.

In the present paper, we describe the application of quasi-elastic and electrophoretic light scattering techniques to the investigation of mixtures of PEAA with a second membrane-forming lipid, dioleoylphosphatidylcholine (DOPC, **2b**). DOPC and DPPC differ in several important respects as a result of the presence of the cis double bond at C_9 in each of the acyl chains of DOPC. The most readily apparent difference lies in the temperatures (T_m) of the main bilayer phase transitions; T_m = 41 °C for DPPC versus −22 °C for DOPC.[11] This difference in melting behavior brings with it the important practical consequence that DPPC exists in the highly ordered L'_β phase at room temperature, whereas DOPC at room temperature is in an L_α phase characterized by nearly liquidlike acyl chain disorder. One might anticipate that such differences in acyl chain packing would be reflected in the nature of the membrane reorganization that accompanies polyelectrolyte adsorption on DPPC or DOPC. We explore in the following sections the structural reorganization of DOPC vesicle membranes by PEAA.

Experimental Section

Materials. Dioleoylphosphatidylcholine (DOPC, 99% purity) was purchased from Sigma Chemical Co. and used without purification. 2-Ethylacrylic acid was prepared by alkaline hydrolysis of methyl 2-ethylacrylate and fractionally distilled (bp 52 °C (1 mm Hg)). Radical polymerization of 2-ethylacrylic acid was run in bulk in a sealed tube at 60 °C under N_2, with 0.5 mol % AIBN as initiator. The polymer was dissolved in pyridine and precipitated in aqueous HCl. After it stood overnight, the polymer was collected by filtration and dried in vacuo at 55 °C. The polymer was further purified by ultrafiltration in water; that fraction retained on a membrane filter of molecular weight cutoff 3×10^4 (Amicon Corp.) was used in these experiments. The weight-average molecular weight ($\bar{M}_w$) of the final product was estimated to be $3.6 \times 10^4 \pm 10\%$ by gel permeation chromatography (GPC). The molecular weight was determined relative to poly(ethylene oxide) (PEO) by GPC with a set of two TSK columns (TSK 3000 PW, TSK 5000 PW, Toyo Soda Mfg. Co.) and a differential refractometer. Calibration was based on a set of nine PEO samples of narrow molecular weight distribution, with average molecular weights in the range from monomer to 10^6. The polymer concentration was about 0.2 wt % in a phosphate buffer solution (0.034 M, pH 8) that contained 0.3 M NaCl.

Sample Preparation. Samples were prepared in aqueous $Na_2HPO_4/NaH_2PO_4/NaCl$ solutions (sodium phosphate buffers) of constant ionic strength (50 mM unless otherwise noted) or in 50 mM Tris-HCl buffers. All buffer solutions were prepared from doubly distilled, deionized water. Chloroform solutions of DOPC were air-dried and the lipid was then dispersed by vortex agitation in buffer at room temperature. Sample solutions were incubated for at least 1 h before filtration (Millex-HA filters, Millipore Corp., 0.45-μm pore size) at room temperature. Samples were filtered directly into 10-mm-diameter cylindrical cuvettes for QELS measurements or into the sample chamber for ELS measurements. All sample containers were thoroughly cleaned with doubly distilled water before use.

Quasi-Elastic Light Scattering. The average hydrodynamic radii of polymers and phospholipid vesicles in solution were obtained from the autocorrelation functions (ACFs) of the intensity of scattered light measured in a quasi-elastic light scattering spectrometer of fairly standard design. The scattering cell, containing a sample solution, was situated in a vat in which the temperature was stabilized at 25 °C by a circulating water bath. Light scattered by the sample from an incident laser beam (Ar ion laser, λ = 514.5 nm, power ca. 100 mW) was detected by a photomultiplier tube mounted on a movable arm usually set at a scattering angle of 90°. A pulse amplifier/discriminator transformed the photomultiplier output into standard logic pulses used by the digital correlator (Langley Ford Instruments division of Coulter Electronics, Inc., Model 1096, 256 channels) to compute the photon count ACF. The ACF was approximately an exponentially decaying function as a result of diffusive motion of scatterers in the sample. The average decay rate, $\bar{\Gamma}$, was determined by a second cumulant fit to the correlation function.[12] $\bar{\Gamma}$ is related to the diffusion coefficient, D, and the scattering vector, $\mathbf{q}$, by

$$\bar{\Gamma} = 2Dq^2 \tag{1}$$

and

$$q = |\mathbf{q}| = \frac{4\pi n}{\lambda} \sin(\theta/2) \tag{2}$$

where n is the refractive index of solvent, λ is the wavelength of incident light in vacuo, and θ is the scattering angle between the incident and scattered light. An average hydrodynamic radius of the particles, R_H, was calculated from the measured diffusion coefficient, D, by using the Stokes-Einstein equation:

$$D = kT/6\pi\eta R_H \tag{3}$$

where k is Boltzmann's constant, T is the absolute temperature, and η is the solvent viscosity. Information concerning the particle size distribution was obtained by a more detailed analysis; Provencher's program CONTIN[13,14] was used to perform the inverse Laplace transform of the ACF.

Electrophoretic Light Scattering. The surface charge densities of vesicles and vesicle–polymer particles were derived from measurements of the electrophoretic mobility in solution. By Henry's law,[15] the observed electrophoretic mobility of a spherical particle of total charge Ze and radius r immersed in a solution containing small counterions can be expressed as

$$\mu = \frac{Ze}{6\pi\eta r} \frac{X(\kappa r)}{1 + \kappa r} \tag{4}$$

where e is the elementary electron charge (4.8×10^{-10} esu) and η is the solvent viscosity (poise). Henry's function $X(\kappa r)$ is sigmoidal in shape, increasing monotonically from unity for $\kappa r \lesssim 1$ to a maximum of 1.5 for $\kappa r \gg 1$. The distribution of counterions

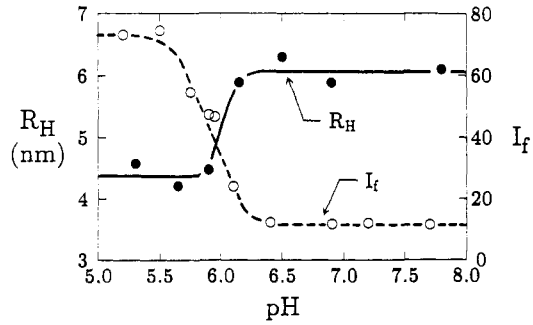

Figure 1. Conformational transition of PEAA upon pH variation. (●) Hydrodynamic radius of PEAA (R_H); 0.5 mg/mL PEAA in 50 mM Tris-HCl buffer (pH 7.8); pH varied by 1 N HCl. (○) Fluorescence intensity (I_f) (arbitrary units); PEAA 1 mg/mL + pyrene 5 μM in 50 mM Tris-HCl buffer.

about a central charged particle is characterized by the Debye–Hückel parameter, κ (cm^{-1}):

$$\kappa = (8\pi N_A e^2 I/1000dkT)^{1/2} \quad (5)$$

where N_A is Avogadro's number, I is the ionic strength of the solution (molar), d is the low-frequency dielectric constant of the solvent (d_{water} = 81), k is Boltzmann's constant, and T is the absolute temperature. For large particles ($\kappa r \gg 1$), Henry's law may be written in the form used in our analysis:

$$\mu = \sigma/\eta\kappa \quad (6)$$

where σ is the average charge density on the surface of the particle (esu/cm^2). Note that particle radius does not appear in eq 6.

Mobility measurements in vesicle–polymer systems were made by using a Doppler electrophoretic light scattering apparatus (DELSA) from Langley Ford Instruments division of Coulter Electronics, Inc. The DELSA instrument combines the techniques of electrophoresis in solution and laser Doppler velocimetry[16-18] to obtain the velocity of particles moving under the influence of an applied electric field and thus the mobility. Simultaneous analysis at four light scattering angles provided by the instrument was useful for removing ambiguities which might otherwise have occurred due to the different scattering and diffusive properties associated with particles of different size contained within each sample.

The sample preparation procedure was the same as for QELS measurements. The inner surface of the DELSA sample chamber was coated with methylcellulose to minimize surface charge and electroosmosis[19] by a procedure adapted from Smith and Ware.[20] About 30 min were allowed for the solution to reach equilibrium, which was determined by observing the constancy of the conductivity. Directional flow in the chamber was avoided by alternating the sign of the applied electric field and pausing between data collection periods to dissipate joule heating.[16]

Results and Discussion

Conformational Transition of PEAA. Evidence for the pH-dependent conformational transition of poly(2-ethylacrylic acid) has been provided by titrimetric[7,8] and spectroscopic[5,9] techniques. For example, acidification of PEAA solutions that contain micromolar amounts of pyrene—either codissolved or bound to the polymer chain—causes a large increase in the intensity of the pyrene fluorescence.[5] The rise in fluorescence intensity occurs at ca. pH 6.1, although its precise position and shape depend on ionic strength and polymer molecular weight.[21] Similar observations had been reported previously for poly(methacrylic acid) (PMAA) by Chen and Thomas[22] and were interpreted as evidence for conformational collapse to a globular polymer coil in which pyrene is solubilized and in which pyrene–water contacts are reduced.

The results shown in Figure 1 are consistent with such an interpretation for PEAA. The figure reports the pH-dependence of the pyrene emission intensity (I_f) at 375 nm for solutions of 5 μM pyrene in Tris-buffered aqueous

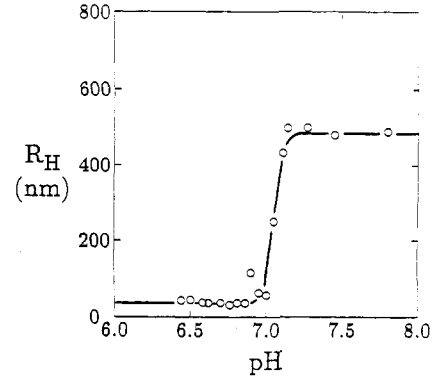

Figure 2. pH dependence of average vesicle size in the presence of PEAA in sodium phosphate buffer. DOPC (10 μg/mL) + PEAA (10 μg/mL) in 50 mM sodium phosphate buffer. Measurements were made after 1 h incubation at 25 °C.

PEAA (1 mg/mL polymer). Also shown is the hydrodynamic radius (R_H) of PEAA dissolved at a concentration of 0.5 mg/mL in similar buffers. Under these conditions, one observes a sharp decrease in R_H between pH 6.2 and 5.9, nearly coincident with the rise in I_f. We find R_H to be ca. 6 nm at high pH versus ca. 4.4 nm below pH 5.9. Although we are unaware of previous measurements of R_H for PEAA, these results appear to be reasonable in comparison with two recent studies of PMAA. Sedlák et al.[23] report R_H = 3.3 nm for neutral PMAA of $\bar{M}_w = 3.0 \times 10^4$ dissolved in salt-free aqueous solutions at a concentration of 36.6 mg/mL, and Pleštil and co-workers[24] observed an increase in the radius of gyration from 4.0 to 7.5 nm upon half-ionization of PMAA of $\bar{M}_w = 2.1 \times 10^4$ dissolved at 40 mg/mL in aqueous solutions in the absence of salt.

QELS Studies of DOPC–PEAA Mixtures. Dispersion of DOPC in phosphate-buffered solutions of PEAA gives rise to vesicular lipid aggregates at pH >7.0. Under our conditions (cf. Experimental Section) the average hydrodynamic radius of such aggregates is determined to be ca. 500 nm. Similar preparations in mildly acidic (pH 6.4–6.9) buffers afford much smaller particles; $R_H \approx 40$ nm at low pH (Figure 2). The change in particle size is remarkably abrupt, in that the transition is complete between pH 7.0 and 7.1 under the conditions of Figure 2.

The values of R_H plotted in Figure 2 were calculated by the application of eq 1 and 3 to the observed autocorrelation functions. Analysis of these same functions by Provencher's inverse Laplace transform method [by means of the computer program CONTIN[13]] allows an estimate of the *distribution* of particle sizes in each sample. At pH 7.27, the decay rate distribution is unimodal and consistent with an average particle radius of ca. 500 nm (Figure 3). At transition (pH 7.05), the distribution is bimodal with one peak at 470 nm and a second at 31 nm; the number of particles in the population at 31 nm (larger Γ) is actually much greater. (This apparent contradiction arises because a larger particle scatters light much more strongly than a small one and the amplitudes in Figure 3 are based on scattered intensity.) At pH 6.81, the distribution is again unimodal and centered at R_H = 37 nm. The pH dependence of the particle size distribution is strongly suggestive of a two-state process of vesicle reorganization; one finds in the sample at a given pH either large (ca. 500 nm) or small (ca. 40 nm) lipid particles. Within the pH range of the transition, both populations are present, but under no circumstances have we observed a *continuous* decrease in radius with decreasing pH.

The average hydrodynamic radius observed in acidic aqueous DOPC/PEAA mixtures is dependent upon a number of experimental parameters, including incubation

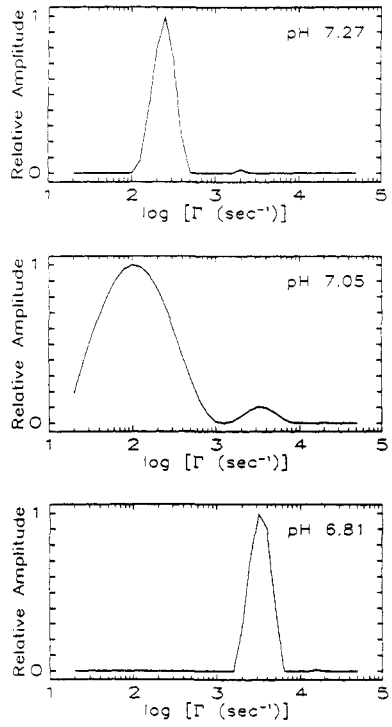

Figure 3. Vesicle size distribution at different pH's. Γ is the autocorrelation function decay rate and is inversely proportional to particle radius (see eq 1 and 3).

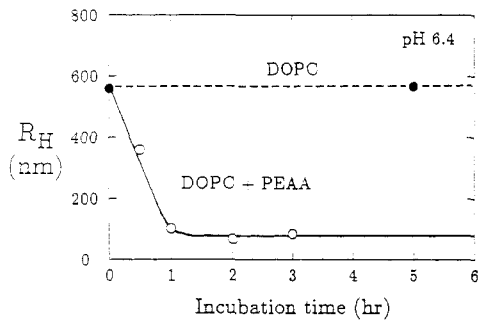

Figure 4. Incubation time dependence of average vesicle size. (●) DOPC 10 μg/mL; (○) DOPC 10 μg/mL + PEAA 10 μg/mL; each phospholipid sample was dissolved in 50 mM sodium phosphate buffer (pH 6.4), incubated at room temperature for the time indicated, and then filtered (Millipore Millex-HA, 0.45-μm pore size) directly into a cuvette for QELS size measurements.

time, buffer composition, ionic strength, and polymer–lipid stoichiometry. Figure 4 shows the time dependence of the size of lipid aggregates incubated with PEAA at pH 6.4. The average hydrodynamic radius drops from ca. 560 to 60–80 nm within 1 h at room temperature; longer incubation leads to no further decrease in particle size. DOPC vesicles incubated in *polymer-free* phosphate buffer solutions, on the other hand, are stable with respect to size reduction under these conditions (Figure 4).

Acidification of vesicle suspensions initially prepared at high pH leads to membrane reorganization and particle size reduction on a similar time scale. Figure 5 shows the average hydrodynamic radius of DOPC aggregates suspended initially in aqueous PEAA at pH 8.0 and then acidified to pH 6.2. R_H drops from an initial value of about 520 nm to a final value of 90–100 nm, with a characteristic "decay time" of approximately 30 min at pH 6.2. We have not explored the pH dependences of the rate of membrane reorganization or of the final particle size.

Figure 6 illustrates the effect of ionic strength on the "critical" pH for membrane reorganization in phosphate-

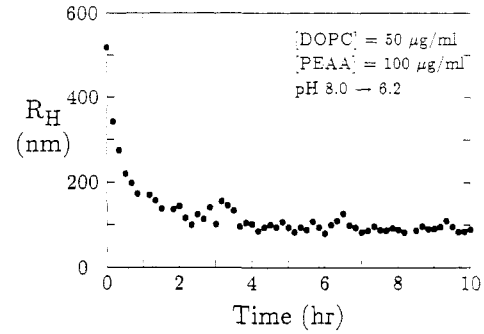

Figure 5. Kinetics of vesicle disruption following a pH change. 50 μg/mL of DOPC and 100 μg/mL of PEAA were dissolved in 50 mM sodium phosphate buffer. At t = 0, a small volume of 50 mM monobasic sodium phosphate solution was added to induce a pH change from 8.0 to 6.2.

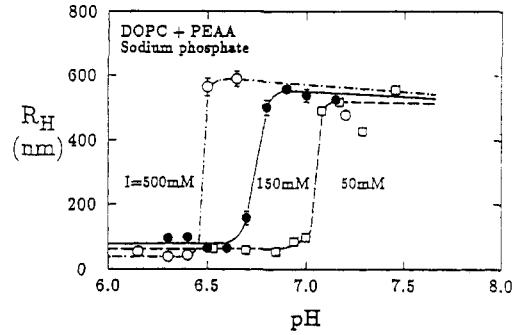

Figure 6. Effect of ionic strength, I, on the pH dependence of the average vesicle size. DOPC (10 μg/mL) + PEAA (10 μg/mL) in sodium phosphate buffer: (○) I = 500 mM; (●) I = 150 mM; (□) I = 50 mM. Because of sample-to-sample variation, any apparent systematic ionic strength dependence of average vesicle size far from the transition pH is not significant.

buffered solutions of PEAA. Increasing the ionic strength from 50 to 500 mM depresses the pH of the midpoint of the structural transition from 7.1 to 6.5. This is consistent with our observations by potentiometric titration[21] and fluorescence intensity[25] that the effect of added salt is to lower the conformational transition pH of PEAA. Similar effects of ionic strength on the conformational transition of poly(methacrylic acid) have also been reported.[26] Increasing ionic strength extends to lower pH the range of stability of the expanded coil of PEAA, probably by a mechanism which may be understood as follows. Polymer-bound carboxylic acid functions will deprotonate as pH increases. The increased charge repulsion on the polyion causes an expansion of the weakly acid PEAA chain, resulting in less conformational entropy. The loss of entropy reduces acidity causing the pK_a of the polyacid to be higher than that of the monomer, as is confirmed experimentally.[21] At high ionic strength, polyion charge is screened, decreasing the conformational entropy loss, with the result that deprotonation occurs at a lower pH, closer to the pK_a of the monomer. Thus in solutions of high ionic strength, the chain remains ionized and hydrated as the pH is depressed to below 7.1. Adsorbtion, dehydration and conformational collapse are then deferred until the pH is depressed further, with the result that the polyelectrolyte-driven membrane reorganization is displaced to lower pH.

Membrane reorganization in acidic mixtures of DOPC and PEAA requires a minimum concentration of the polyelectrolyte. Figure 7 shows the results of a series of experiments in which DOPC at a fixed concentration (100 μg/mL) was treated with various amounts of PEAA at pH 6.3. At a polymer:lipid ratio ≥0.1 by weight, the particle size is effectively reduced; R_H < 100 nm. On the other

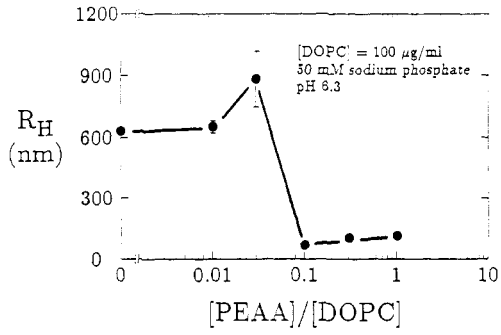

Figure 7. Dependence of average vesicle size on PEAA–DOPC ratio. DOPC (100 μg/mL) in 50 mM sodium phosphate buffer (pH 6.3).

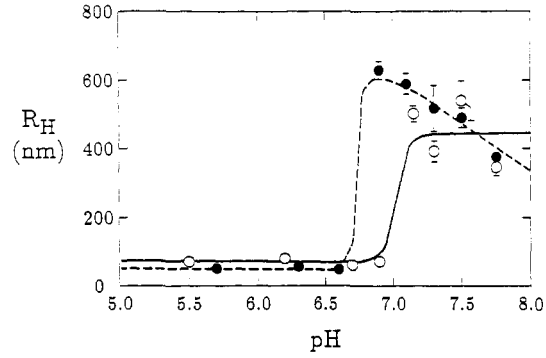

Figure 8. pH dependence of phospholipid vesicle size in Tris-HCl buffer: (○) DOPC (10 μg/mL) + PEAA 50 (μg/mL) in 50 mM Tris-HCl buffer; (●) DOPC (10 μg/mL) + PEAA (10 μg/mL) in the same buffer. Error bars represent only the variation (one standard deviation) within several runs on the same sample preparation. Sample to sample variations are somewhat larger. We are unable to say whether the intact vesicles are increasing, decreasing, or constant in size in the high-pH region.

hand, at PEAA:DOPC ≤ 0.03, one observes no reduction in R_H. The implication is that the small (R_H < 100 nm) aggregates must contain a minimum fraction—perhaps 10% by weight—of PEAA. We are presently determining the compositions of a variety of mixed aggregates of phosphatidylcholine and PEAA.[27]

The pH at which membrane reorganization occurs is sensitive not only to ionic strength but to the *identity* of the buffer ions as well. Figure 8 shows the variation of R_H with pH in DOPC suspensions prepared in solutions of PEAA buffered with Tris-HCl, rather than sodium phosphate. Comparison of Figures 6 and 8 reveals that the transition pH is depressed by ca. 0.4 units in the ammonium (Tris) buffer. The data also demonstrate the sensitivity of the critical pH to the polymer–lipid stoichiometry, in that a 5-fold increase in the concentration of PEAA raises the critical pH from 6.7 to 7.1 under otherwise constant conditions. This shift in critical pH with rising polymer concentration must reflect an increase in the amount of PEAA bound to the membrane at a fixed pH.

ELS Studies of DOPC–PEAA Mixtures. Electrophoretic light scattering yields a plot of the total intensity of light scattered by particles of a given mobility versus the mobility (μ). In our samples, μ is proportional to the surface charge density (σ) (cf. Experimental Section). Typical mobility spectra for DOPC vesicle suspensions are shown in Figure 9. The spectra imply a highly peaked distribution of mobilities; there is undoubtedly a wide range of particle sizes present, but one value of surface charge per unit area is dominant.

Figure 10 shows the pH dependence of DOPC vesicle mobility in phosphate buffer and in phosphate-buffered PEAA. In the polymer-free suspension, mobility decreases

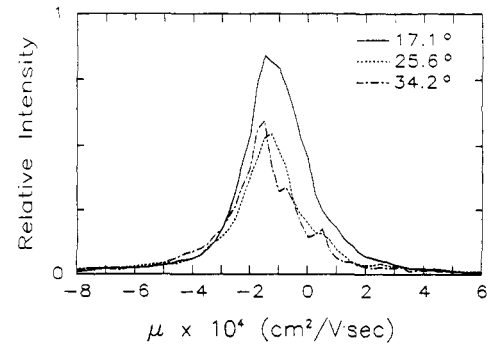

Figure 9. Typical mobility (μ) spectra of a DOPC vesicle suspension. DOPC (10 μg/mL) + PEAA (10 μg/mL) in 50 mM sodium phosphate buffer (pH 7.0). The three spectra were measured simultaneously at the three scattering angles indicated.

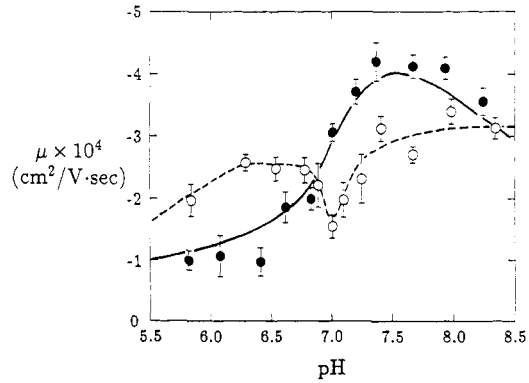

Figure 10. pH dependence of phospholipid vesicle mobility (μ): (○) DOPC (10 μg/mL) + PEAA 10 (μg/mL) in 50 mM sodium phosphate buffer; (●) DOPC (10 μg/mL) in the same buffer.

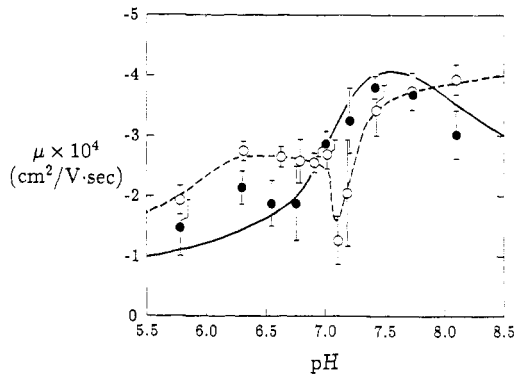

Figure 11. pH dependence of phospholipid vesicle mobility (μ): (○) DOPC 10 (μg/mL) + PEAA 30 (μg/mL) in 50 mM sodium phosphate buffer; (●) DOPC (10 μg/mL) in the same buffer.

rather abruptly as the pH is depressed from 7.4 to 6.4 and remains relatively constant at higher and lower pH. These results are generally consistent with those of Schlieper and co-workers[28] and reflect the development of increased negative surface charge at high pH through the adsorption of negative ions (either hydroxide or phosphate) from the basic solution. In the polymer solution, the mobility varies with pH in quite a different manner, in that the decline in μ between pH 7.5 and 7.0 is followed by a rising mobility upon further acidification. Thus μ reaches a minimum value of 1.5×10^{-4} cm²/V·s at pH 7.0. When the polymer concentration is increased 3-fold (Figure 11), the pattern of mobility variation is similar, except that the local minimum in μ is better defined and displaced by 0.1 unit to higher pH.

For solution conditions of the mobility measurements, the Debye–Hückel parameter κ is estimated from eq 5 to be 7.23×10^6 cm^{-1}, so that for vesicles of 600-nm radius,

$\kappa r \approx 434 \gg 1$. For 60-nm spheres, $\kappa r \approx 43 \gg 1$. In each case then, the simplified form of Henry's law for large particles (eq 6) can be used to estimate surface charge density. At pH 7.5–8.5, the observed mobility 3×10^{-4} $cm^2/V \cdot s$ leads to an estimate of $\sigma = 1.21 \times 10^{13}$ e/cm^2 for DOPC suspended in a 10 $\mu g/mL$ solution of PEAA. If one assumes a value of 60 $Å^2$ for the surface area per molecule of DOPC,[29] the average number of of surface charges per lipid molecule is ca. 0.07. If the surface charge arises from adsorption of buffer or solvent anions, this value should decrease as the pH is reduced, as indeed it does in the polymer-free suspension. In aqueous PEAA, however, the surface charge rises again at low pH, with the rise in σ nearly superimposed on the drop in R_H (cf. Figures 2 and 10). Because PEAA remains substantially ionized at pH 7,[30] the rise in σ must signal the increase in polymer adsorption that drives vesicle reorganization and forces the decrease in particle size.

Conclusions

The combined application of quasi-elastic and electrophoretic light scattering techniques to the polyelectrolyte-driven reorganization of phosphatidylcholine vesicle membranes leads to the following conclusions.

1. PEAA undergoes an abrupt conformational transition from an expanded, hydrophilic coil at high pH to a much more compact, hydrophobic structure in acidic aqueous solutions. The pH of the conformational transition may be determined either by QELS or by photophysical methods that involve codissolved pyrene as a probe; the transition pH is found to be nearly identical by these methods.

2. Acidification of aqueous mixtures of DOPC and PEAA results in a decrease in the average hydrodynamic radius (R_H) from 600 to ca. 40 nm. The pH of the structural transition varies with polymer concentration, buffer composition, and ionic strength. The transition appears to be a two-state process, in that analysis of the particle size distribution shows the coexistence of large and small particles. Under no circumstances have we observed a continuous variation in particle size with pH.

3. Vesicle membrane reorganization in this system occurs on a time scale of 30–60 min and requires a polymer:lipid ratio ≥ 0.1.

4. Vesicle membrane reorganization is coincident with an increase in polymer adsorption, as reported by a rise in electrophoretic mobility at pH ≤ 7.0.

It is of some interest to compare these results with those reported previously for mixtures of PEAA with the saturated lipid DPPC.[10] In that case, membrane reorganization produced a mixed micellar aggregate of $R_H = 5.5$ nm. The DOPC vesicle membrane, in contrast, adopts a geometry in which R_H is reduced only to 40–50 nm, a value inconsistent with micellar organization. We suggest that the 40-nm aggregate is vesicular and that the decrease in particle size arises from an increase in membrane curvature induced by preferential association of PEAA with the outer leaflet of the bilayer. Such a result would be analogous to the observation that certain mixtures of short- and long-chain phosphatidylcholines will spontaneously form small unilamellar vesicles, presumably with some asymmetry in the transmembrane distribution of each of the lipid components.[31] That DOPC remains vesicular under conditions that convert DPPC to mixed micellar form would suggest a reluctance on the part of the unsaturated lipid to adopt the higher degree of surface curvature characteristic of micellar organization. This in turn is consistent with the larger cross-sectional area requirements of the unsaturated acyl chains of DOPC.

Acknowledgment. This work was supported by an NSF Presidential Young Investigator Award to D. A. Tirrell and by Army Research Office Grant DAAL03-88-K-0038 to D. A. Tirrell and K. H. Langley. We thank Langley Ford Instruments Division of Coulter Electronics, Inc., for the use of DELSA electrophoretic light scattering apparatus. Polymer molecular weights were determined for us by Dr. U. K. O. Schröder. The fluorescence results presented in Figure 1 were provided by K. A. Borden.

Registry No. PEAA, 62607-09-4; DOPC, 10015-85-7.

References and Notes

(1) Bangham, A. D.; Standish, M. M.; Watkins, J. C. *J. Mol. Biol.* **1965**, *13*, 238.
(2) Seki, K.; Tirrell, D. A. *Macromolecules* **1984**, *17*, 1692.
(3) Tirrell, D. A.; Takigawa, D. Y.; Seki, K. *Ann. N.Y. Acad. Sci.* **1985**, *446*, 237.
(4) Devlin, B. P.; Tirrell, D. A. *Macromolecules* **1986**, *19*, 2465.
(5) Borden, K. A.; Eum, K. M.; Langley, K. H.; Tirrell, D. A. *Macromolecules* **1987**, *20*, 454.
(6) Tirrell, D. A. *J. Controlled Release* **1987**, *6*, 15.
(7) Fichtner, F.; Schonert, H. *Colloid Polym. Sci.* **1977**, *255*, 230.
(8) Joyce, D. E.; Kurucsev, T. *Polymer* **1981**, *22*, 415.
(9) Sugai, S.; Nitta, K.; Ohno, N.; Nakano, H. *Colloid Polym. Sci.* **1983**, *261*, 159.
(10) Borden, K. A.; Eum, K. M.; Langley, K. H.; Tan, J. S.; Tirrell, D. A.; Voycheck, C. L. *Macromolecules* **1988**, *21*, 2649.
(11) Lichtenberg, D.; Robson, R. J.; Dennis, E. A. *Biochim. Biophys. Acta* **1983**, *737*, 285.
(12) Koppel, D. E. *J. Chem. Phys.* **1972**, *57*, 4814.
(13) Provencher, S. W. *Makromol. Chem.* **1979**, *180*, 201.
(14) Provencher, S. W.; Hendrix, J.; Maeyer, L. de; Paulussen, N. *J. Chem. Phys.* **1978**, *69*, 4273.
(15) Tanford, C. *Physical Chemistry of Macromolecules*; Wiley: New York, 1961.
(16) Ware, B. R.; Haas, D. D. In *Fast Methods in Physical Biochemistry and Cell Biology*; Sha'afi, R. I., Fernandez, S. M., Eds.; Elsevier: Amsterdam, 1983; p 173.
(17) Watrasiewicz, B. M.; Rudd, M. J. *Laser Doppler Measurements*; Butterworths: London, 1976.
(18) Drain, L. E. *The Laser Doppler Technique*; Wiley: New York, 1961.
(19) Vanderhoff, J. W.; Micale, F. J.; Krumrine, P. H. In *Electrophoresis '78*; Catsimpoolas, N., Ed.; Elsevier: Amsterdam, 1978; p 405.
(20) Smith, B. A.; Ware, B. R. In *Contemporary Topics in Analytical and Clinical Chemistry*; Hercules, D. M., Hieftje, G. M., Snyder, L. R., Evenson, M. A., Eds.; Plenum: New York, 1978; Vol. 2, p 46.
(21) Schröder, U. K. O.; Tirrell, D. A. *Macromolecules* **1989**, *22*, 765.
(22) Chen, T.; Thomas, J. K. *J. Polym. Sci.* **1979**, *17*, 1103.
(23) Sedlák, M.; Koňák, Č.; Štěpánek, P.; Jakeš, J. *Polymer* **1987**, *28*, 873.
(24) Pleštil, J.; Ostanevich, Yu. M.; Bezzabotonov, V. Yu.; Hlavatá, D.; Labský, J. *Polymer* **1986**, *27*, 839.
(25) Borden, K. A.; Tirrell, D. A., unpublished results.
(26) Mandel, M.; Leyte, J. C.; Stadhouder, M. G. *J. Phys. Chem.* **1967**, *71*, 603.
(27) Borden, K. A.; Tirrell, D. A., unpublished results.
(28) Schlieper, P.; Medda, P. K.; Kaufmann, R. *Biochim. Biophys. Acta* **1981**, *644*, 273.
(29) Tanford, C. *The Hydrophobic Effect*, 2nd ed.; Wiley: New York, 1980.
(30) Schröder, U. K. O.; Tirrell, D. A., unpublished results.
(31) Gabriel, N. E.; Roberts, M. F. *Biochemistry* **1984**, *23*, 4011.